Biol. Cybern. 74, 255–261 (1996)

Biological Cybernetics

Modeling motor cortical operations by an attractor network of stochastic neurons

A. V. Lukashin[1,2], B. R. Amirikian[1,2], V. L. Mozhaev[1,2], G. L. Wilcox[3], A. P. Georgopoulos[1,2]

[1] Brain Sciences Center 11B, Department of Veterans Affairs Medical Center, One Veterans Drive, Minneapolis, MN 55417, USA
[2] Department of Physiology and Neurology, University of Minnesota Medical School, Minneapolis, MN 55455, USA
[3] Department of Pharmacology, University of Minnesota Medical School, and Minnesota Supercomputer Institute, University of Minnesota, Minneapolis, MN 55455, USA

Received: 21 February 1995/Accepted in revised form: 19 September 1995

Abstract. Understanding the neural computations performed by the motor cortex requires biologically plausible models that account for cell discharge patterns revealed by neurophysiological recordings. In the present study the motor cortical activity underlying movement generation is modeled as the dynamic evolution of a large fully recurrent network of stochastic spiking neurons with noise superimposed on the synaptic transmission. We show that neural representations of the learned movement trajectories can be stored in the connectivity matrix in such a way that, when activated, a particular trajectory evolves in time as a dynamic attractor of the system while individual neurons fire irregularly with large variability in their interspike intervals. Moreover, the encoding of trajectories as attractors ensures high stability of the ensemble dynamics in the presence of synaptic noise. In agreement with neurophysiological findings, the suggested model can provide a wide repertoire of specific motor behaviors, whereas the number of specialized cells and specific connections may be negligibly small if compared with the whole population engaged in trajectory retrieving. To examine the applicability of the model we study quantitatively the relationship between local geometrical and kinematic characteristics of the trajectories generated by the network. The relationship obtained as a result of simulations is close to the '2/3 power law' established by psychophysical and neurophysiological studies.

1 Introduction

The data obtained from recording the activity of motor cortical cells in the brain of behaving animals can often be interpreted using population vector analysis (see Georgopoulos 1991; Georgopoulos et al. 1993 for a review). Although individual cells possess a preferred direction, their activities are broadly tuned with respect to the direction of arm movement and, therefore, the generation of movement depends upon the activity of the whole ensemble. The population coding hypothesis (Georgopoulos et al. 1983, 1986) suggests that contributions from individual neurons sum vectorially to produce the neuronal population vector and that this is an appropriate measure of the ensemble's directional tendency. Indeed, it was found that the population vector accurately predicts the direction of limb movement in space under a variety of conditions (Georgopoulos 1991; Georgopoulos et al. 1993). As a motor action evolves in time, neuronal population vectors can be calculated over short successive time intervals. Attaching these vectors tip-to-tail yields a neural-vector trajectory that is thought to be a motor cortical representation of the movement to be made (Georgopoulos et al. 1988; Schwartz 1993, 1994).

In general, any computational algorithm, including directional operations in the motor cortex, can be reproduced by many set of network architectures, models of individual neurons and learning rules. A critical test of any biologically plausible model of motor cortical processing is how well it accounts for discharge patterns observed in neurophysiological recordings. In the present paper an ensemble of motor cortical cells performing directional operations is modeled by a fully recurrent neural network consisting of stochastic spiking neurons. The model shows how irregular series of spikes can be combined together to produce an accurate representation of the ongoing movement in terms of neural-vector trajectories. We concentrate on a particular type of movement control: the generation and performance from memory of learned movement trajectories such as drawing simple curves. The key idea is that the cortical representation of a specific motor skill can be stored in the set of connections between neurons so that, after activation, it unfolds in time as a *dynamic attractor* of the system. We demonstrate that this approach guarantees high robustness of the dynamic behavior with respect to

Correspondence to: A. V. Lukashin

superimposed noise. The properties of individual neurons as well as the spatial and temporal characteristics of the trajectories generated by the network are in close quantitative agreement with the corresponding experimental data.

2 Neural network model

As in other cortical areas (Softky and Koch 1993), the firing of the motor cortical cells is nearly consistent with a stochastic process: that is, for a given mean firing rate, highly variable interspike intervals are observed (Taira and Georgopoulos 1993). Therefore, the basic element of an adequate model should be a neuron with similar firing characteristics. To describe a spiking neuron, we use a phenomenological model much like that suggested in Gerstner et al. (1993a). The spike generation process obeys stochastic dynamics in discrete time: for the ith neuron, the firing probability during one time step between t and $t + \tau_s$ ($\tau_s = 1$ ms), given the membrane potential $u_i(t)$ at time t, is defined as:

$$p[t + \tau_s | u_i(t)] = \tau_s V_{max} \tfrac{1}{2}\{1 + \tanh[u_i(t)]\} \quad (1)$$

This expression provides a nonlinear sigmoidal dependence of the firing probability on the instantaneous value of the membrane potential. The probability ranges between zero and some maximal value, which is given by the parameter $V_{max} = 65$ impulses per second (imp/s). We used two different ways to incorporate refractoriness into the model: (i) by adding an absolute refractory period after each spike (Gerstner et al. 1993a) and (ii) by allowing an exponential dependence of the firing probability on the time since the previous spike. The results are scarcely affected by the method of incorporation of refractoriness; in fact the data presented below use (ii).

Neurons modeled as described above are combined into a large fully recurrent network consisting of M units. The probability of firing (1) is determined by the membrane potential, which is the sum of two terms: $u_i(t) = u_i^{ext}(t) + u_i^{syn}(t)$. The external input $u_i^{ext}(t)$ is enabled for only a short period of time (25 ms) and serves to activate network dynamics. The activation period is followed by a self-sustained network dynamics. After the external signal is disabled, the probability of firing is driven strictly by the synaptic input $u_i^{syn}(t)$ from all other neurons in the network. To calculate the synaptic signal entering the ith neuron during one time step τ_s we use the following expression:

$$u_i^{syn}(t) = \tau_s \sum_j^M w_{ij}[1 + \xi_{ij}(t;\sigma)]\varepsilon(t - t_j^{last}) \quad (2)$$

where w_{ij} is a weight of the synaptic connection from the jth to the ith neuron (positive for an excitatory and negative for an inhibitory synapse), and $\xi_{ij}(t;\sigma)$ is the gaussian noise of zero mean and standard deviation σ. The instantaneous values of the noise for different ij-pairs are uncorrelated. The response function ε in (2) describes the time course of the signal received by neuron i from neuron j. We assume that, if a second presynaptic spike arrives during the residual effect of a previous spike at the same synapse, the postsynaptic signal does not increase above the level assigned for a single spike. Therefore, the response function depends only upon the difference $\Delta t = t - t_j^{last}$, where t_j^{last} is the time when the very last spike appeared in the jth neuron. The specific expression for the ε function is the same as suggested in Gerstner et al. (1993a): $\varepsilon(\Delta t) = (\Delta t/\tau_\varepsilon^2)\exp(-\Delta t/\tau_\varepsilon)$, where τ_ε is the response time constant ($\tau_\varepsilon \sim 2$–3 ms in routine calculations).

Thus, the output of the network is a set of M spike trains fired by M neurons. By analogy with the experimental approach (Georgopoulos et al. 1988; Schwartz 1993, 1994), the dynamic evolution of the network's outcome is interpreted as the generation of the neural-vector trajectory in the following manner. Each neuron is assigned a preferred direction $\mathbf{C}_i$ ($i = 1, \ldots, M$) in two-dimensional space: $\mathbf{C}_i = (\cos\alpha_i, \sin\alpha_i)$, where α_i is the preferred direction angle. The assignment of the preferred direction implies that the ith unit should fire maximally for movements making in the direction $\mathbf{C}_i$. The whole dynamics is divided into time bins of equal length T (25 ms), and the combined activity of the ensemble at the kth time bin is represented by the neuronal population vector:

$$\mathbf{P}(k) = \frac{1}{MT}\sum_i^M V_i(k)\,\mathbf{C}_i \quad (3)$$

where $V_i(k)$ is the activity of the ith neuron at the kth time bin, i.e., the number of spikes fired by this neuron during the time interval $(k-1)T < t < kT$. Adding the population vectors tip-to-tail yields the radius vector $\mathbf{R}(k) = \mathbf{P}(1) + \cdots + \mathbf{P}(k-1) + \mathbf{P}(k)$ that defines the kth point at the *neural-vecotr trajectory*.

It was suggested in our previous paper (Lukashin et al. 1994) that neural-vector trajectories of different shapes can be stored in, and generated by, largely overlapping networks with fixed connection strengths. The idea is that each memorized trajectory (or class of trajectories) is generated by a neural subset consisting of two parts: (i) a large 'core' part that is shared by, and engaged with, all kind of trajectories, and (ii) a relatively small part that is specific for, and engaged with, only a particular class of trajectories. The activation of the core part together with one of specialized parts (while other specialized parts are inhibited) results in the generation of trajectory that corresponds to the activated specialized part. The weights of connections between the core units do not carry information about specific trajectories. All information about specific trajectories is stored in the weights of connections between specialized units, and in feedforward and feedback connections between the specialized units and the core part. Due to these connections the core part reveals specific dynamic behavior and, therefore, distinguishes different tasks. In other words, the output of the whole network is provided by the activity of the large core part, whereas the small part serves to specify a particular dynamic behavior of the whole system. In the present paper we use the same overlapping network architecture.

3 Neural-vector trajectories as attractors

In this section we demonstrate that the network of stochastic spiking neurons can store and retrieve neural-vector trajectories of different shapes as dynamic attractors of the system. We dwell on the consideration of simple attractors such as fixed points and limit cycles. In terms of trajectory generation, fixed points correspond to straight lines of different directions and limit cycles may correspond, for example, to clockwise or counterclockwise circular trajectories.

It is important to emphasize the following fact with respect to the construction of the connectivity matrix ensuring a desired dynamic behavior of the network. Since the network's dynamics is driven entirely by intra-network connections, the relevant information about preferred directions of individual neurons must also be encoded in the connectivity matrix. This means that the weight of a particular connection, w_{ij}, must be correlated with the presumed preferred directions, α_i and α_j, of the involved neurons. Experimental findings (Georgopoulos et al. 1993) and results of previous modeling (Lukashin and Georgopoulos 1994) suggest that the strength of connection of a neuron pair tends to be negatively correlated with the difference between their preferred directions. On the basis of this fact, together with the desired tuning properties of the neurons (see below), we choose the following form of the connectivity matrix:

$$w_{ij}^{xy} = a^{xy} \cos(\alpha_i - \alpha_j + \varphi^{xy}) \tag{4}$$

where the coefficients a^{xy} and phase shifts φ^{xy} are the parameters to be adjusted in order to obtain the trajectory of a desired shape. The superscript x indicates which part of the network – core ($x = c$) or specific ($x = s$) – the ith neuron belongs to. The superscript y indicates the same for the jth neuron. The preferred directions α_i ($i = 1, \ldots, M$) are assigned as follows. In the core part of the network, as well as in the specialized parts, the neurons are grouped in clones (columns) of 1000 units each. All neurons belonging to the same clone are assigned the same preferred direction. The preferred directions of the clones within the core part of the network are uniformly distributed. The preferred directions of the clones within a specialized part are also uniformly distributed. This form of the connectivity matrix makes it possible to store and retrieve a wide spectrum of trajectories of different shapes.

Examples of dynamic behavior of the network, underlying three different attractors (straight lines, clockwise, and counterclockwise circles), are depicted in Fig. 1. In each case the dynamics is induced by the short-lasting (25 ms) activation of one of the specialized parts of the network together with the common core part of the network. The number of neurons in the core part of the network $N = 200 \times 10^3$ (200 clones of 1000 neurons each). The weights of connections within this part are given by (4), with $a^{cc} = 3.5 \times 10^{-4}$, $\varphi^{cc} = 0$. The core part of the network is engaged during generation of any kind of trajectory. The specificity of the ensemble dynamics is encoded in the weights of connections within the specialized parts [parameters a^{ss} and φ^{ss} in (4)] and in the weights of connections between specialized parts and the core part of the network [parameters a^{cs}, a^{sc} and φ^{cs}, φ^{sc} in (4)].

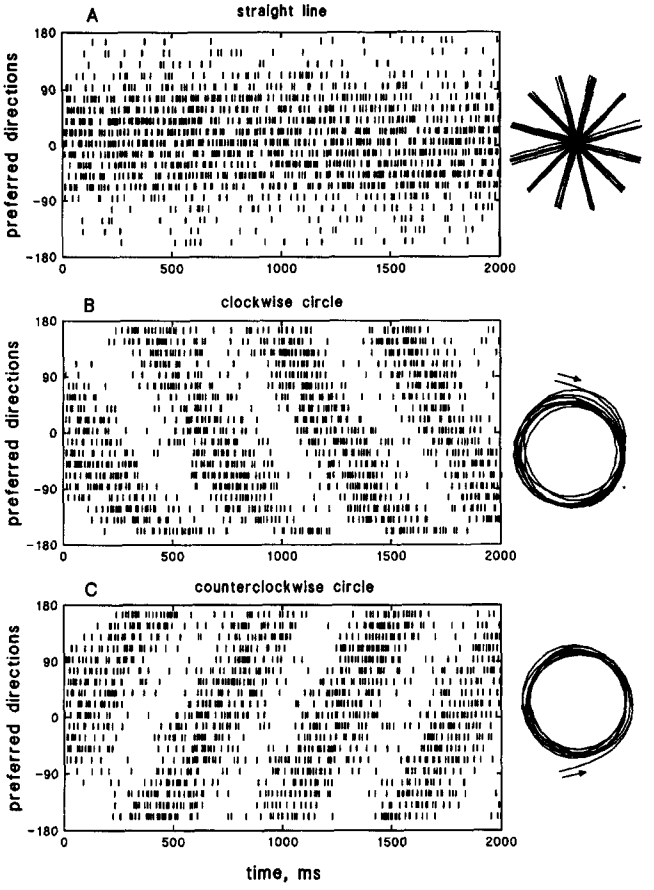

Fig. 1A–C. Spike trains and trajectories generated by the network. *Rasters* show spike trains for 19 core neurons selected from the ensemble of 2×10^5 units. Each *horizontal row* of bars represents the spike train for one neuron. The *bars* mark the spiking time. The neurons are ordered along the vertical axis in accordance with their preferred direction angles. Corresponding neural-vector trajectories are shown to the right of each raster. Raster **A** illustrates the representative activity of the network during generation of a straight-line trajectory (one of 72 trajectories drawn to the right of the raster). For this raster the preferred direction angles are calculated relative to the direction of movement. Rasters **B** and **C** demonstrate the representative activity of the network generating the clockwise and counterclockwise circular trajectories respectively. In both cases the angle of value zero corresponds to the horizontal direction from left to right

The dynamics shown in Fig. 1A corresponds to the following choice of the specialized connections (4): $a^{ss} = 3.5 \times 10^{-4}$, $\varphi^{ss} = 0$; $a^{cs} = a^{sc} = 1.05 \times 10^{-3}$, $\varphi^{cs} = \varphi^{sc} = 0$. The number of neurons in the specialized part $n = 12 \times 10^3$ (12 clones of 1000 neuron each). This neural subset (the core part plus the specialized part) can store and retrieve 12 straight-line trajectories, and retrieving a particular direction of the trajectory depends on the initial direction given by the short-lasting external input. The cluster of trajectories shown in Fig. 1A was activated by 72 uniformly distributed initial directions. Correspondingly, a stable clockwise circular trajectory (Fig. 1B)

can be obtained if, in addition to the core part, another specialized part of the network is engaged, and the specialized connections are given by parameters (4) $a^{ss} = 1.75 \times 10^{-3}$, $\varphi^{ss} = -\pi/2$; $a^{cs} = a^{sc} = 1.05 \times 10^{-3}$, $\varphi^{cs} = \varphi^{sc} = 0$. Finally, the generation of counterclockwise circular trajectory (Fig. 1C) can be provided by the specialized part with the same set of parameters, except that the phase shift φ^{ss} should be positive: $\varphi^{ss} = \pi/2$. Regularly repeated excitation of individual neurons followed by an inhibition is clearly seen for the circular movement (Fig. 1B, C).

The angular velocity of circular neural-vector trajectories is modulated by parameters a^{ss} and φ^{ss} determining the weights of connections between neurons belonging to the specialized part of the network. The combination $\{a^{ss} = 1.75 \times 10^{-3}, \varphi^{ss} = \pm \pi/2\}$, which corresponds to the trajectories shown in Fig. 1B and C, is chosen because it provides the angular velocity of the rotation of neuronal population vector equal to 430 deg/s that is close to the experimentally measured value of about 400 deg/s (Georgopoulos et al. 1993). A variation of parameters a^{ss} and φ^{ss} retains a circular shape of the neural-vector trajectory (except for the case $\varphi^{ss} = 0$, which obviously corresponds to a straight-line trajectory with the zero value of angular velocity). The following results clarify the sensitivity of angular velocity to parameters a^{ss} and φ^{ss}: combinations $\{a^{ss} = 1.75 \times 10^{-3}, \varphi^{ss} = \pm \pi/12\}$ and $\{a^{ss} = 1.75 \times 10^{-3}, \varphi^{ss} = \pm \pi/4\}$ result in angular velocities equal to 190 and 320 deg/s, respectively; and combinations $\{a^{ss} = 0.875 \times 10^{-3}, \varphi^{ss} = \pm \pi/2\}$ and $\{a^{ss} = 3.50 \times 10^{-3}, \varphi^{ss} = \pm \pi/2\}$ result in angular velocities equal to 230 and 940 deg/s, respectively.

In fact, the neural-vector trajectories shown in Fig. 1 exemplify the simplest types of attractor dynamics such as straight lines and circles, for which the weights of synaptic connections can be given in an explicit form (4). The connectivity matrices that store more complex patterns of neuronal activity could be found using, for example, a hebbian learning procedure suggested by Gerstner et al. (1993b) or by means of a special variant of the simulated annealing algorithm developed in Lukashin et al. (1996).

The spike trains presented in Fig. 1 demonstrate a large variability of interspike intervals for the firing of individual neurons. Indeed, our calculations show that even for the straight-line trajectories, the coefficient of variation, which is the ratio of the standard deviation to the mean of the interspike interval, ranges between 0.5 and 1. This high level of variability is consistent with the common situation observed for real cortical cells (Softky and Koch 1993). It is important to note that, while individual units fire irregularly, the dynamic behavior of the network as a whole is highly stable. Both features of the model – the variability of interspike intervals and the stability of the ensemble's behavior – are in agreement with experimental observations in the motor cortex (Georgopoulos et al. 1983, 1986, 1988; Taira and Georgopoulos 1993).

The attractor dynamics depicted in Fig. 1 is ensured by the intra-network connections, and it may last until a new external signal comes. For example, a short-lasting signal can inhibit the currently engaged specialized part and activate another one. Then the whole network will be switched to the generation of another trajectory. The property of the model that is noteworthy is the robustness of the self-sustained dynamics with respect to the presence of noise in the synaptic transmission (2). This is illustrated in Fig. 2 by the example of progressive degradation of an attractor by increasing noise. To quantify the influence of noise, we calculated the mean radius of curvature for a trajectory generated at different noise levels and plotted this value versus the standard deviation of noise σ (Fig. 2). Typical trajectories generated at several noise levels are also shown in Fig. 2. Both representations indicate that the ability of the network to perform a memorized task is only weakly affected by the noise until the standard deviation σ approaches the value $\sigma \sim 1$, when the 'noise' becomes comparable to the 'signal' [see (2)].

4 'Inhomogeneity' of the network and tuning curves

In this section we show that the suggested model fits two important properties of real ensemble of motor cortical

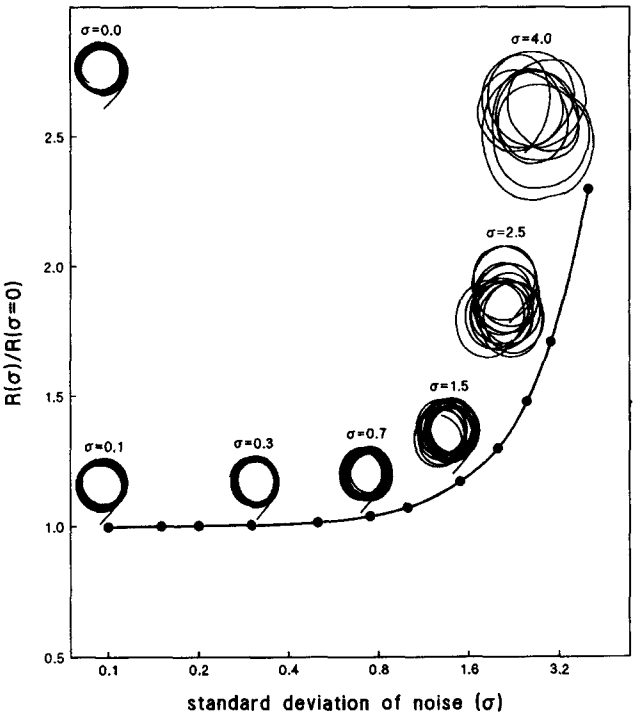

Fig. 2. Performance of the network in the presence of gaussian noise superimposed on the synaptic transmission. The ratio of the mean radius of curvature of the trajectory, $R(\sigma)$, to the corresponding value of the zero noise, $R(\sigma = 0)$, is plotted as a function of the standard deviation of noise, σ (*connected points*). Note the logarithmic scale of the abscissa. Each *point* corresponds to the average of the mean radius over 10 trajectories generated with the same σ. The error bars are hidden within the size of the points. *Curves* represent typical trajectories generated by the network with the indicated values of σ. The curve drawn in the *upper left-hand corner* is a trajectory generated with zero noise

cells performing directional operations. First, only a small number of cells is very specific to a particular trajectory, whereas a large number of cells is engaged during performance of many different tasks (Hocherman and Wise 1991; Smyrnis et al. 1992; Ashe et al. 1993). Second, the dependence of the mean firing rate of a cell on the direction of movement (the tuning curve) is coarse and can be approximated by a smooth cosine-like function (Georgopoulos et al. 1983). Obviously, the network without specialized connections cannot generate a specific trajectory from memory. The larger the relative contribution of specific connections to the whole connectivity matrix, the easier it is to store and retrieve specific set of trajectories. We refer to this contribution of specialized parts as the 'inhomogeneity' of the network and quantify it by introducing a parameter $\gamma = W^{\text{specific}}/W^{\text{total}}$, where W^{total} is the sum of absolute values of the connection strengths (4) taken over the whole ensemble and W^{specific} is the same for the specialized connections. Hence, the problem we tried to solve is to construct an optimal network with inhomogeneity reduced to a minimum while retaining the desired dynamic behavior of the network as well as an appropriate shape of tuning curves.

We have analyzed this problem for the case of straight-line attractors (Fig. 3). The three clusters of trajectories at the top of Fig. 3 demonstrate how the retrieving ability of the network depends on the inhomogeneity γ if the numbers of neurons in the specialized part, n, and in the core part of the network, N, are fixed ($n = 12 \times 10^3$ and $N = 200 \times 10^3$). The network retrieves memorized trajectories (12 straight lines) only if the parameter γ exceeds a critical value ($\gamma \approx 0.17$ in the present case). This is an optimal inhomogeneity of the network. Evaluated as described above, the resulting optimal values of inhomogeneity γ are plotted in Fig. 3A as a function of N for two sizes of the specialized part: $n = 12 \times 10^3$ and $n = 8 \times 10^3$. In both cases, the optimal inhomogeneity is seen to decrease as N increases, obeying a dependence N^{-1}, and the smaller n is, the lower is the optimal inhomogeneity. In particular, these results indicate that, in the real motor cortex, the relative number of specialized cells and specific connections may be negligibly small if compared with the whole neuronal ensemble engaged in generation of a memorized movement. The tuning properties of the neurons in the optimal network are shown in Fig. 3B. As for the real motor cortical cells, each neuron's output varies approximately as the cosine of the difference between direction of movement and its own preferred direction. The range of variability of the firing rate (5–65 imp/s) is the same as observed in experiments (Taira and Georgopoulos 1993). It is important to note that this tuning function is not imposed externally, but emerges as a result of intra-network interactions during the dynamics. The curves drawn in Fig. 3A represent only the lower bounds of the inhomogeneity that is needed to provide the performance of the network. The retrieving properties of the network together with the desired shape of the tuning curves are guaranteed everywhere over the bound.

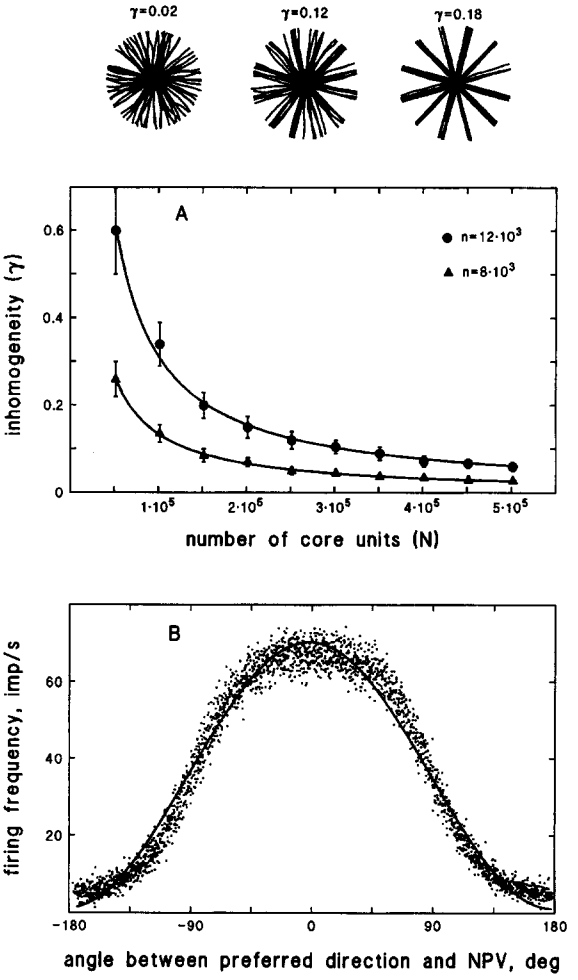

Fig. 3A, B. Optimal inhomogeneity of the network and tuning properties of individual neurons. The three clusters of curves at the *top* are the trajectories generated by the network with different values of the parameter of inhomogeneity γ (see text) as indicated over each cluster. There are 72 trajectories in each cluster that correspond to 72 uniformly distributed initial directions. The number of neurons n in the specialized part is 12×10^3 (12 clones of 10^3 units each). This specialized part provides the capability of generating 12 different strainght-line attractors. The number of units in the core part N is 200×10^3. The connectivity matrix for the right cluster, corresponding to the optimum performance of the network, is the same as for the dynamic behavior shown in Fig. 1A (see Sect. 3). **A** The optimal value of γ is plotted versus the number of the core units, N, for the number of specialized units $n = 12 \times 10^3$ (*circles*) and $n = 8 \times 10^3$ (*triangles*). The *continuous curves* are fits by regressions using the law N^{-1}. The data were obtained by averaging over 10 trials. **B** The dependence of the mean firing rate of the core units on the difference between the preferred direction and the direction of movement represented by the direction of the neuronal population vector (NPV). The data were obtained for the optimal network generating the right-hand cluster of trajectories shown at the *top*. *Points* are the firing rates of 200 units (one unit from each clone) calculated for 12 directions of movement. The *continuous curve* is an approximation by the cosine function $a + b\cos(x)$, where $a = 35.0$ imp/s, $b = 34.5$ imp/s

5 The '2/3 power law'

The neural-vector trajectory is thought to be a motor cortical representation of the trajectory of the hand (Georgopoulos et al. 1988; Schwartz 1993, 1994). Up to this point we have dealt with the shapes of trajectories.

The kinematic characteristics can also be considered in the framework of the suggested model. With respect to the applicability of the model to the real motor cortex, it is of special interest to examine quantitatively the geometrical and kinematic characteristics of curved neural-vector trajectories and to compare them with experimental data.

By definition, the ratio of the instantaneous angular velocity, A, to the tangential velocity, V, is equal to the curvature, C, at each point on a trajectory: $A/V = C$. Therefore, tracing trajectories with variable curvature can be accomplished only if A and V co-vary with curvature. In general, this co-variation could be arbitrary within the relation $A/V = C$. Nevertheless, psychophysical studies of curved hand movements indicate that the velocities A and V obey invariant rules: $A = kC^{\beta}$, $V = kC^{\beta-1}$, where k and β are constants, and $\beta \approx 2/3$ (Viviani and Terzuolo 1982; Lacquaniti et al. 1983; Massey et al. 1992). This relationship has been termed the '2/3 power law'. It has been hypothesized (Massey et al. 1992) that this law reflects a neural constraint: the tighter the curvature of a trajectory, the longer is the time needed to rotate the neuronal population vector. Indeed, the '2/3 power law' has recently been well documented for experimentally measured neural-vector trajectories (Schwartz 1994). Below we demonstrate that our model shows the same relation between geometrical and kinematic characteristics.

Since a neural-vector trajectory is constructed by attaching the time sequence of the neuronal population vectors tip-to-tail, the length of the neuronal population vector is a measure of the tangential velocity of movement, V, averaged over the duration of the time bin. Correspondingly, the angle between the directions of two adjacent vectors is a measure of the angular velocity, A. To find a correlation between the geometrical and kinematic characteristics of the neural-vector trajectories generated by the network we used the following procedure. As usual, the weights of connections inside the core part were fixed, whereas the remaining connections were adjusted to obtain circles of different radius or complex figures with variable curvature. Some of these figures are drawn at the top of Fig. 4. For each trajectory generated, the angular velocity A was calculated step by step along a trajectory as the angle between two adjacent neuronal population vectors divided by the time bin T.. Corresponding values of the curvature C were calculated as the same angles divided by the lengths of the neuronal population vector. Finally, the length of the neuronal population vector was used as the tangential velocity V at corresponding points on a trajectory. Since the neuronal population vector has dimensionally 'imp/s' rather than 'length/s', the latter correspondence is valid only within each class of trajectory (circles, ellipses, spirals, etc.). Therefore, for each class of trajectory the unit length, λ, may be chosen arbitrarily. We chose the values of λ in such a way that all curved trajectories fall within the same range of curvature variability. The angular and tangential velocities are plotted as functions of the curvature in Fig. 4A and B, respectively. It is seen that the results can be approximated by the power law $A = kC^{\beta}$,

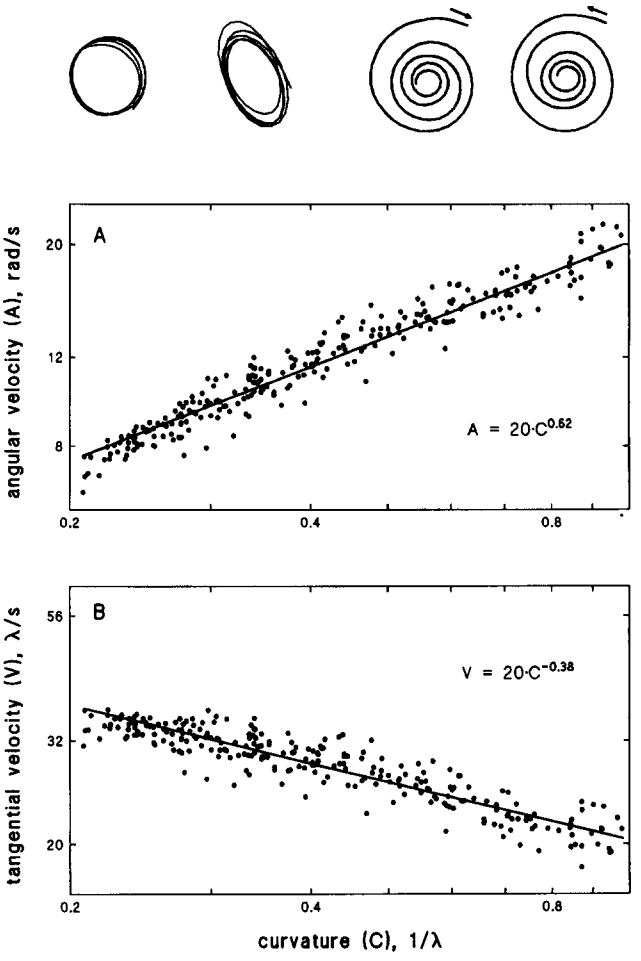

Fig. 4A, B. Power law for angular (**A**) and tangential (**B**) velocities. Four examples of the trajectories analyzed are shown at the *top* of the figure. The method of calculation is described in the text. The angular and the tangential velocities are plotted versus the curvature on a log-log scale. The *points* represent the data for 20 circles of different radius and for trajectories with the variable curvature shown on the top. The values A, V and C for the circles were obtained by averaging over each trajectory. The *continuous lines* are the best fit approximated by the power law $A = kC^{\beta}$, $V = kC^{\beta-1}$. The best fitting values are $k = 20$, $\beta = 0.62$.

$V = kC^{\beta-1}$ with the exponent $\beta = 0.62$; this is close to the experimentally measured value $\beta \approx 2/3$.

The data presented in Fig. 4 were obtained for a particular set of the basic parameters of the model. Of course, varying the parameters may result in a change in the exponent β. Nevertheless, it is important that the suggested model is able to reproduce an experimentally observed relationship between geometrical and kinematic characteristics of trajectories; this was not apparent *a priori*. We believe these results support the neural-constraint hypothesis (Massey et al. 1992) concerning the origin of the '2/3 power law'.

6 Conclusions

The hypothesis that multiple motor skills may be stored in, and generated by, overlapping neural networks has

been entertained in our previous paper (Lukashin et al. 1994). In the present study we use this idea concerning the network architecture and show that motor cortical representation of learned movements may be stored and generated as dynamic attractors of the network. The model provides high stability of the ensemble dynamics, in spite of the fact that both the firing of individual neurons and synaptic transmission are stochastic processes. The model considered in the present paper possesses the following characteristics that are biologically relevant. First, the basic properties of discharge patterns for individual neurons closely parallel those of motor cortical cells: large variability of interspike intervals and cosine-like tuning curves (Georgopoulos et al. 1993; Taira and Georgopoulos 1993). Second, all properties of the network emerge as a result of the correlated intranetwork interactions; this is in accord with an experimental observation that the intra-cortical connections provide the major signal arriving at any neuron (Douglas et al. 1989; Keller 1993). Third, although each particular trajectory is generated by a large ensemble of neurons only a small number of neurons and connections is specific to a particular trajectory; this feature of the model is consistent with neurophysiological findings (Hocherman and Wise 1991; Smyrnis et al. 1992; Ashe et al. 1993). Fourth, the model can generate curved trajectories obeying the '2/3 power law'; this relationship has been well documented in psychophysical and neurophysiological studies. Finally, the interplay of modeling approach and recording experiments reported in the present paper suggests an experimentally testable hypothesis concerning an attractor nature of the motor cortical representation of memorized movement.

Acknowledgements. This research was supported by United States Public Health Service Grant PSMH48185 to A.P.G., a contract from the Office of Naval Research to A.P.G. and A.V.L., grants of supercomputer resources from Minnesota Supercomputer Institute to A.P.G. and G.L.W., and Minnesota Supercomputer Institute Research Scholar to B.R.A.

References

Ashe J, Taira M, Smyrnis N, Pellizzer G, Georgakopoulos T, Lurito JT, Georgopoulos AP (1993) Motor cortical activity preceding a memorized movement trajectory with an orthogonal bend. Exp Brain Res 98:118–130

Douglas RJ, Martin KAC, Whitteridge D (1989) A canonical microcurcuit for neocortex. Neural Comput 1:480–488

Georgopoulos AP (1991) Higher order motor control. Annu Rev Neurosci 14:361–377

Georgopoulos AP, Caminiti R, Kalaska JF, Massey JT (1983) Spatial coding of movement: a hypothesis concerning the coding of movement by motor cortical population. Exp Brain Res [Suppl 7]: 327–336

Georgopoulos AP, Schwartz AB, Kettner RE (1986) Neuronal population coding of movement direction. Science 233:1416–1419

Georgopoulos AP, Kettner RE, Schwartz AB (1988) Primate motor cortex and free arm movement to visual targets in three-dimensional space. II. Coding of the direction of movement by a neuronal population. J Neurosci 8:2928–2937

Georgopoulos AP, Taira M, Lukashin AV (1993) Cognitive neurophysiology of the motor cortex. Science 260:47–52

Gerstner W, Ritz R, Hemmen JL van (1993a) A biologically motivated and analytically soluble model of collective oscillations in the cortex. I. Theory of weak locking. Biol Cybern 68:363–374

Gerstner W, Ritz R, Hemmen JL van (1993b) Why spikes? Hebbian learning and retrieval of time-resolved excitation patterns. Biol Cybern 69:503–505

Hocherman S, Wise SP (1991) Effects of hand movement path on motor cortical activity in awake, behaving rhesus monkeys. Exp Brain Res 83:285–302

Keller A (1993) Intrinsic synaptic organization of the motor cortex. Cerebral Cortex 3:430–441

Lacquaniti F, Terzuolo C, Viviani P (1983) The law relating the kinematic and figural aspects of drawing movements. Acta Physiol 54:115–130

Lukashin AV, Georgopoulos AP (1994) A neural network for coding of trajectories by time series of neuronal population vectors. Neural Comput 6:19–28

Lukashin AV, Wilcox GL, Georgopoulos AP (1994) Overlapping neural networks for multiple motor engrams. Proc Natl Acad Sci USA 91:8651–8654

Lukashin AV, Wilcox GL, Georgopoulos AP (1996) Modeling of directional operations in the motor cortex: a noisy network of spiking neurons is trained to generate neural-vector trajectories. Neural Networks, in press

Massey JT, Lurito JT, Pellizzer G, Georgopoulos AP (1992) Three dimensional drawing in isometric conditions: relation between geometry and kinematics. Exp Brain Res 88:685–690

Schwartz AB (1993) Motor cortical activity during drawing movements: population representation during sinusoid tracing. J Neurophysiol 70:28–36

Schwartz AB (1994) Direct cortical representation of drawing. Science 265:540–542

Smyrnis N, Taira M, Ashe J, Georgopoulos AP (1992) Motor cortical activity in a memorized delay task. Exp Brain Res 92:139–151

Softky WR, Koch C (1993) The highly irregular firing of cortical cells is inconsistent with temporal integration of random ESPSs. J Neurosci 13:334–350

Taira M, Georgopoulos AP (1993) Cortical cell types from spike trains. Neurosci Res 17:39–45

Viviani P, Terzuolo CA (1982) Trajectory determines movement dynamics. Neuroscience 7:431–437